



HAL
open science

Synthesis of Tris(arylphosphite)-ligated Cobalt(0) Complexes $[\text{Co}_2(\text{CO})_6\text{P}(\text{OAr})_3]_2$, and their Reactivity towards Phenylacetylene and Diphenylacetylene

Isabelle Jourdain, Michael Knorr, Lukas Brieger, Carsten Strohmann

► **To cite this version:**

Isabelle Jourdain, Michael Knorr, Lukas Brieger, Carsten Strohmann. Synthesis of Tris(arylphosphite)-ligated Cobalt(0) Complexes $[\text{Co}_2(\text{CO})_6\text{P}(\text{OAr})_3]_2$, and their Reactivity towards Phenylacetylene and Diphenylacetylene. *Advances in Chemical Research*, 2020, 2 (4), 10.21926/acr.2004009 . hal-03025150

HAL Id: hal-03025150

<https://hal.science/hal-03025150v1>

Submitted on 28 Aug 2021

HAL is a multi-disciplinary open access archive for the deposit and dissemination of scientific research documents, whether they are published or not. The documents may come from teaching and research institutions in France or abroad, or from public or private research centers.

L'archive ouverte pluridisciplinaire **HAL**, est destinée au dépôt et à la diffusion de documents scientifiques de niveau recherche, publiés ou non, émanant des établissements d'enseignement et de recherche français ou étrangers, des laboratoires publics ou privés.



Distributed under a Creative Commons Attribution 4.0 International License

Research article

Synthesis of Tris(arylphosphite)-ligated Cobalt(0) Complexes $[\text{Co}_2(\text{CO})_6\{\text{P}(\text{OAr})_3\}_2]$, and their Reactivity towards Phenylacetylene and Diphenylacetylene¹

Isabelle Jourdain ^{1,*}, Michael Knorr ^{1,*}, Lukas Brieger ², Carsten Strohmann ²

1. Institut UTINAM UMR 6213 CNRS, Université Bourgogne Franche-Comté, 16, Route de Gray, 25030 Besançon, France; E-Mails: isabelle.jourdain@univ-fcomte.fr; michael.knorr@univ-fcomte.fr

2. Anorganische Chemie, Technische Universität Dortmund, Otto-Hahn Straße 6, 44227 Dortmund, Germany; E-Mails: lukas.brieger@tu-dortmund.de; carsten.strohmann@tu-dortmund.de

* **Correspondence:** Isabelle Jourdain and Michael Knorr; E-Mails: isabelle.jourdain@univ-fcomte.fr; michael.knorr@univ-fcomte.fr

Academic Editor: Maxim L. Kuznetsov

Special Issue: [Coordination Chemistry and Metal Complexes](#)

Advances in Chemical Research
2020, volume 2, issue 4
doi:10.21926/acr.2004009

Received: September 07, 2020

Accepted: November 06, 2020

Published: November 25, 2020

Abstract

The dinuclear complexes $[\text{Co}_2(\text{CO})_6\{\text{P}(\text{OAr})_3\}_2]$ (**1a**, Ar = Ph; **1b**, Ar = *o*-Tol) were prepared and reacted with $\text{PhC}\equiv\text{CH}$ and $\text{PhC}\equiv\text{CPh}$ to yield dimetallatetrahedranes $[\{(\text{ArO})_3\text{P}\}(\text{OC})_2\text{Co}-\text{Co}(\mu\text{-RC}\equiv\text{CPh})(\text{CO})_2\{\text{P}(\text{OAr})_3\}]$ (**3a**, Ar = Ph, R = H; **3b**, Ar = *o*-Tol, R = H; **3c**, Ar = Ph, R = Ph; **3d**, Ar = *o*-Tol, R = Ph). The main reaction of diphenylacetylene was accompanied by a side reaction, leading to the dissociation of a $\text{P}(\text{OAr})_3$ ligand for the formation of mono(phosphite) complexes $[\{(\text{ArO})_3\text{P}\}(\text{OC})_2\text{Co}-\text{Co}(\mu\text{-PhC}\equiv\text{CPh})(\text{CO})_3]$ (**2b**, R = Ph; **2d**, R = *o*-Tol). The crystal structures of **1b**, **3a**, and **3d** were determined along with that of the mono(phosphite) complex $[\{(\text{PhO})_3\text{P}\}(\text{OC})_2\text{Co}-\text{Co}(\mu\text{-PhC}\equiv\text{CPh})(\text{CO})_3]$ **2b**.

¹ This article is dedicated to Prof. Jacques Amaudrut on the occasion of his 80th birthday



© 2020 by the author. This is an open access article distributed under the conditions of the [Creative Commons by Attribution License](#), which permits unrestricted use, distribution, and reproduction in any medium or format, provided the original work is correctly cited.

Keywords

Cobalt; alkyne; phosphite; crystal structure; dimetallatetrahedrane; metal-metal bond

1. Introduction

The organometallic reaction of dicobalt octacarbonyl with alkynes to yield dicobaltatetrahedranes $[\text{Co}_2(\text{CO})_6(\mu\text{-RC}\equiv\text{CR}')] [1, 2]$ has been extensively studied ever since its first discovery in the fifties [3]. The studies are not only aimed to understand the synthetic aspects, spectroscopic and structural characterization of these cage-like species but also to utilize these compounds as precursors for further modifications. The Nicholas reaction is an example, where a dicobalt hexacarbonyl-stabilized propargylic cation $[\text{Co}_2(\text{CO})_6(\mu\text{-R}_1\text{C}\equiv\text{C-CR}_2\text{R}_3)]^+$, generated by the reaction of $[\text{Co}_2(\text{CO})_8]$ with a propargylic ether $\text{R}_1\text{C}\equiv\text{C-C(OR)R}_2\text{R}_3$ or an alkynol $\text{R}_1\text{C}\equiv\text{C-C(OH)R}_2\text{R}_3$, followed by subsequent treatment with a Lewis acid, reacts with a nucleophile (Nuc) to form $[\text{Co}_2(\text{CO})_6(\mu\text{-R}_1\text{C}\equiv\text{C-C(Nuc)R}_2\text{R}_3)] [4-7]$. The mild oxidation of such functionalized dimetallatetrahedranes results in the formation of substituted alkynes, which finds application in organic chemistry [8]. The Pauson-Khand reaction is, however, the most common transformation, in which $[\text{Co}_2(\text{CO})_8]$ is reacted with an alkyne, alkene, and carbon monoxide to form an α,β -cyclopentenone [9-16]. This [2+2+1] cycloaddition is often used in synthetic organic chemistry. The addition of bridging diphosphines, such as bis(diphenylphosphino)methane (dppm) or bis(diphenylphosphino)amine (dppa), stabilizes the moderately labile metal-metal bond of the air-sensitive $[\text{Co}_2(\text{CO})_8]$ complex [7, 13, 17-19]. Besides, more stabilization may be achieved by the replacement of one or more carbonyls by monodentate P-donors such as PR_3 and P(OR)_3 . A literature-survey revealed considerable studies on the dicobalt species $[\text{Co}_2(\text{CO})_{n-x}\{\text{P(OR)}_3\}_x] [20]$ coordinated with up to four alkyl phosphite ligands and their reaction with alkynes [21-27]. However, the structural characterization of $[\text{Co}_2(\text{CO})_{n-x}\{\text{P(OAr)}_3\}_x]$ complexes is limited, comprising of the structures of $[\text{Co}_2(\text{CO})_6\{\text{P(OPh)}_3\}_2]$ and $[\text{Co}_2(\text{CO})_6\{\text{P(O-2,4-}t\text{-Bu}_2\text{C}_6\text{H}_3)_3\}_2]$ alone [28, 29]. These compounds were probed for hydroformylation studies. However, there are no reports on the structural features of aryl phosphite-substituted dimetallatetrahedranes $\{[(\text{ArO})_3\text{P}]\{\text{OC}\}_2\text{Co-Co}(\mu\text{-RC}\equiv\text{CR})(\text{CO})_2\{\text{P(OAr)}_3\}\}$. In this study on the reactivity of metal-metal bonded dinuclear complexes with alkynes [30-36], an unknown complex, namely $[\text{Co}_2(\text{CO})_6\{\text{P(OTol-}o\text{)}_3\}_2]$ **1b**, was synthesized along with $[\text{Co}_2(\text{CO})_6\{\text{P(OPh)}_3\}_2]$ **1a** and reacted with phenylacetylene and diphenylacetylene. The resultant Co(0) complexes were characterized in solution by IR and multinuclear NMR spectroscopy as well as four single-crystal X-ray diffraction studies.

2. Materials and Methodologies

2.1 General procedure

All the reactions were performed in Schlenk tubes under an argon atmosphere. Based on previous literature, the solvents were dried and distilled before use, which were further stored under argon. The reagents diphenylacetylene, phenylacetylene, triphenyl phosphite, tri-*o*-tolylphosphite, and dicobaltoctacarbonyl were used as received from Sigma-Aldrich or Acros. The $\text{Co}_2(\text{CO})_6\{\text{P(OPh)}_3\}_2$ complex was prepared as described in the literature [28]. The reactions were

monitored using IR spectroscopy in the $\nu(\text{CO})$ region. The infrared spectra were recorded in solution using the Shimadzu IR Affinity-1 spectrometer or Bruker Vertex 70 FT-IR spectrometer equipped with a Platinum ATR accessory containing a diamond crystal. The standard IR abbreviations used are as follows: s = strong, m = medium, sh = shoulder, vs = very strong, and w = weak. The elemental analyses were performed at Service d'Analyses Élémentaires, UMR 7053 CNRS, Vandoeuvre-Les-Nancy, France. The $^{31}\text{P}\{^1\text{H}\}$, $^{13}\text{C}\{^1\text{H}\}$, and ^1H NMR spectra were recorded in CDCl_3 at 161.99, 100.62, and 400.13 MHz, respectively, using the Bruker Avance 400HD spectrometer. The solvent was used as the standard reference for calibrating the chemical shift. The chemical shift δ is given in ppm and J in Hz. The phosphorus chemical shifts are externally referenced using 85% H_3PO_4 in H_2O . The standard NMR abbreviations used are as follows: br = broad, m = multiplet, s = singlet, d = doublet, and Cq = quaternary carbon.

2.2 Synthesis of the Complexes

$[\text{Co}_2(\text{CO})_6\{\text{P}(\text{OTol-}o)_3\}_2]$ (1b**)** This complex was prepared by following the same procedure as that reported in the literature for the synthesis of $[\text{Co}_2(\text{CO})_6\{\text{P}(\text{OPh})_3\}_2]$ [28]. A mixture of $[\text{Co}_2(\text{CO})_8]$ (1.00 g, 2.93 mmol) and 2.1 eq of $\text{P}(\text{OTol-}o)_3$ (1.90 ml, 6.15 mmol) were stirred in toluene (10 ml) under 90°C . The reaction was monitored using IR spectroscopy. After 3h, the solution was concentrated under vacuum, and the product **1b** was crystallized at 4°C as a reddish-brown solid. About 2.1 g of the product was obtained with a yield of 73%. The calculated values for $\text{C}_{48}\text{H}_{42}\text{Co}_2\text{O}_{12}\text{P}_2$ (990.67) were C, 58.20, and H, 4.27, against which the observed values were C, 58.11, and H, 4.22. The ^1H NMR spectrum showed peaks at δ 2.14 (br, 18H, CH_3) and 7.10-7.29 (m, 24H, Ar). The $^{13}\text{C}\{^1\text{H}\}$ NMR spectrum was found to possess peaks at δ 16.3 (CH_3), 120.7, 125.2, 126.9, 131.6 (CH), 130.4 (C-Me), 149.7 (C-OP), and 199.8 (CO). The $^{31}\text{P}\{^1\text{H}\}$ NMR peak was observed at δ 159.9 (s). The IR (ATR) spectrum showed peaks at 1993 (w) and 1957 cm^{-1} (vs) $\nu(\text{CO})$.

Synthesis of $\{[(\text{ArO})_3\text{P}]\{\text{OC}\}_2\text{Co-Co}(\mu\text{-RC}\equiv\text{CPh})(\text{CO})_2\{\text{P}(\text{OAr})_3\}\}$

$\{[(\text{PhO})_3\text{P}]\{\text{OC}\}_2\text{Co-Co}(\mu\text{-HC}\equiv\text{CPh})(\text{CO})_2\{\text{P}(\text{OPh})_3\}\}$ (3a**) Method a:** The reagent phenylacetylene (21.9 ml, 0.2 mmol) was added to 5 ml solution of $\text{Co}_2(\text{CO})_6\{\text{P}(\text{OPh})_3\}_2$ (182.0 mg, 0.2 mmol) mixed in toluene. The reaction mixture was heated at 60°C . After 2h, the resultant solution was cooled to room temperature prior to reducing its temperature to 4°C . The reddish-brown needles formed on crystallization were collected by filtration. The product yield was found to be 89 %. The observed values for $\text{C}_{48}\text{H}_{36}\text{Co}_2\text{O}_{10}\text{P}_2$ (952.63) were C, 60.38; H, 3.78 against the calculated values of C, 60.52; H, 3.81.

Method b: Prior to the addition of phenylacetylene (32.9 ml, 0.3 mmol), the $[\text{Co}_2(\text{CO})_8]$ complex (100.0 mg, 0.3 mmol) was dissolved in 5 ml of heptane. The solution was stirred overnight at room temperature. To this mixture, 2 eq. of $\text{P}(\text{OPh})_3$ (153 ml, 0.6 mmol) was added and stirred under 80°C . After 4h, the resulting solution was allowed to reach room temperature. The temperature of the mixture was further reduced to 4°C . The resultant reddish-brown needles were collected by filtration. The product yield was found to be 83 %. ^1H NMR: δ 4.57 (br, 1H, CH), 6.90-7.46 (m, 35H, Ar). $^{13}\text{C}\{^1\text{H}\}$ NMR: δ 69.7 (CH), 87.0 (Cq), 121.2, 124.8, 126.6, 128.0, 129.6, 131.9 (CH), 140.0 (Cq), 151.2 (C-OP), 203.8 (CO). $^{31}\text{P}\{^1\text{H}\}$ NMR: δ 153.0 (s). IR (ATR): 2032(s), 1978(vs) $\nu(\text{CO})$. IR (cyclohexane): 2045 (s), 2000 (s), 1992 (s) $\nu(\text{CO})$.

$\{[(o\text{-TolO})_3\text{P}]\{\text{OC}\}_2\text{Co-Co}(\mu\text{-HC}\equiv\text{CPh})(\text{CO})_2\{\text{P}(\text{OTol-}o)_3\}\}$ (3b**)** This derivative was prepared by following the same procedures as described above and was, in turn, isolated as a reddish brown

solid. **Method a**: Yield: 85 %. Calculated values for $C_{54}H_{48}Co_2O_{10}P_2$ (1036.79): C, 62.56; H, 4.67; Observed values for $C_{54}H_{48}Co_2O_{10}P_2$ (1036.79): C, 62.64; H, 4.72. **Method b**: Yield: 81 %. 1H NMR: δ 2.01 (br, 18H, CH_3), 5.04 (br, 1H, CH), 6.90-7.46 (m, 29H, Ar). $^{13}C\{^1H\}$ NMR: δ 16.4 (CH_3), 68.6 (CH), 89.1 (Cq), 120.2, 124.4, 125.6, 126.6, 127.3 (CH), 129.9 (C-Me), 131.4, 131.5, (CH), 139.3 (Cq), 150.0 (C-OP), 203.6 (CO). $^{31}P\{^1H\}$ NMR: δ 148.8 (s). IR (ATR): 2032 (s), 1976 (vs) $\nu(CO)$. IR (cyclohexane): 2045 (s), 1999 (s), 1993(s), 1937 (w) $\nu(CO)$.

[(PhO)₃P](OC)₂Co-Co(μ -PhC \equiv CPh)(CO)₂P(OPh)₃] (3c) This compound was prepared by following the same procedures as described above and was, in turn, isolated as a reddish black solid. **Method a**: Yield: 81 %. Using *method b*, the slow concentration of the mother liquors was achieved resulting in the formation of black needles of **2b** (Yield: 5%). **Method b**: Yield: 86 %. Calculated values for $C_{54}H_{40}Co_2O_{10}P_2$ (1028.72): C, 63.05; H, 3.92; Observed values for $C_{54}H_{40}Co_2O_{10}P_2$ (1028.72): C, 62.85; H, 3.79. 1H NMR: δ 6.65-7.93 (m, Ar). $^{13}C\{^1H\}$ NMR: δ 86.8 (Cq), 121.0, 124.7, 126.2, 128.2, 129.6, 131.1 (CH), 141.6 (Cq), 151.3 (C-OP), 203.1 (CO). $^{31}P\{^1H\}$ NMR: δ 147.4 (s). IR (ATR): 2033 (s), 1981 (vs) $\nu(CO)$. IR (cyclohexane): 2046 (s), 2006 (s), 1994 (s), 1946 (w) $\nu(CO)$.

[(OC)₃Co-Co(μ -PhC \equiv CPh)(CO)₂P(OPh)₃] (2b) Calculated values for $C_{37}H_{25}Co_2O_8P$ (746.44): C, 59.54; H, 3.38; Observed values for $C_{37}H_{25}Co_2O_8P$ (746.44): C, 59.63; H, 3.45. 1H NMR: δ 6.59-7.67 (m, Ar). $^{13}C\{^1H\}$ NMR: δ 89.4 (Cq), 121.0 (d, $^3J_{PC} = 4$ Hz), 125.1, 127.1, 128.7, 129.9, 130.2 (CH), 140.0 (Cq), 151.2 (Cq-O, d, $^2J_{PC} = 9$ Hz), 200.6, 202.5 (CO) $^{31}P\{^1H\}$ NMR: δ 147.0 (s). IR (ATR): 2062 (s), 2017 (s), 2001 (s), 1978 (s) $\nu(CO)$.

[(*o*-TolO)₃P](OC)₂Co-Co(μ -PhC \equiv CPh)(CO)₂P(OTol-*o*)₃] (3d) This compound was prepared by following the same procedures as described above and was further isolated as black-purple plates. **Method a**: Yield: 88 %. The slow concentration of the mother liquors via *method b* afforded **2d** as a brown powder (Yield: 8%). **Method b**: Yield: 86 %. Calculated values for $C_{60}H_{52}Co_2O_{10}P_2$ (1112.89): C, 64.76; H, 4.71; Observed values for $C_{60}H_{52}Co_2O_{10}P_2$ (1112.89): C, 64.64; H, 4.72. 1H NMR: δ 1.89 (br, 18H, CH_3), 6.77-8.04 (m, 34H, Ar). $^{13}C\{^1H\}$ NMR: δ 16.1 (CH_3), 85.8 (Cq), 120.3, 124.1, 126.3, 126.5, 128.3 (CH), 129.7 (C-Me), 130.9, 131.1 (CH), 141.2 (Cq), 150.3 (C-OP), 203.9 (CO). $^{31}P\{^1H\}$ NMR: δ 142.1 (s). IR (ATR): 2033 (s), 1979 (vs) $\nu(CO)$. IR (cyclohexane): 2043 (s), 2000 (s), 1991 (s), 1932 (w) $\nu(CO)$.

[(OC)₃Co-Co(μ -PhC \equiv CPh)(CO)₂P(OTol-*o*)₃] (2d) Calculated values for $C_{40}H_{31}Co_2O_8P$ (788.53): C, 60.93; H, 3.96; Observed values for $C_{40}H_{31}Co_2O_8P$ (788.53): C, 61.09; H, 3.88. 1H NMR: δ 2.12 (br, 9H, CH_3), 6.65-7.66 (m, 22H, Ar). $^{13}C\{^1H\}$ NMR: δ 16.2 (CH_3), 88.7 (Cq), 120.0, 125.5, 126.5, 127.2, 128.6 (CH), 128.6 (C-Me), 131.5, 131.4 (CH), 139.7 (Cq), 149.2 (Cq-O), 200.4, 203.4 (CO). $^{31}P\{^1H\}$ NMR: δ 142.2 (s). IR (ATR): 2062 (s), 2021 (s), 1998 (s) $\nu(CO)$.

2.3 Crystallographic Studies

The crystal structures of the compounds **1b**, **2b**, **3a**, and **3d** were determined using the *Bruker D8 Venture* four-circle diffractometer equipped with a *PHOTON II* CPAD detector by *Bruker AXS GmbH*. The X-ray radiation was generated by the *l μ S/l μ S 3.0* microfocus source (for compound **3a**) Mo ($\lambda = 0.71073$ Å) from *Incoatec GmbH* equipped with *HELIOS* mirror optics and a single-hole collimator by *Bruker AXS GmbH*. The selected crystals of **1b**, **3a**, **2b**, and **3d** were covered with an inert oil (perfluoropolyalkyl ether) and mounted on the *MicroMount* from *MiTeGen*.

The APEX 3 Suite (v.2018.7-2) software integrated with SAINT (integration) and SADABS (adsorption correction) programs by Bruker AXS GmbH were used for data collection. The processing and finalization of the crystal structure were performed using the Olex2 program [37]. The crystal structures were solved by the ShelXT [38] structure solution program using the Intrinsic Phasing option, which were further refined by the ShelXL [39] refinement package using Least Squares minimization. The non-hydrogen atoms were anisotropically refined. The C-bound H atoms were placed in geometrically calculated positions, and a fixed isotropic displacement parameter was assigned to each atom according to the riding-model: C–H = 0.95–0.98 Å with $U_{\text{iso}}(\text{H}) = 1.5U_{\text{eq}}(\text{CH}_3)$ and $1.2U_{\text{eq}}(\text{CH})$ for other hydrogen atoms. In compound **3a**, the hydrogen atom on C1 was located on the difference Fourier map and refined independently. In compound **1b**, two of the three *ortho*-cresyl groups were positionally disordered and refined using free variables. The oxygen atom O4 and carbon atoms C4–C10 were disordered with a ratio of 52:48, while the carbon atoms C18–C24 were disordered with a ratio of 55:45. The carbon atoms C8 and C18 were excluded from the disorder. In compound **2b**, two of the three –OPh groups were positionally disordered. The –OPh group at the P4 atom with the oxygen atom O26 was disordered with a ratio of 77:23. The carbon atom C123 was excluded from the disorder. The –OPh group at the P4 phosphorus atom with the oxygen atom O27 was disordered with a ratio of 83:17. The carbon atom C125 was excluded from the disorder. The crystallographic data and structural refinement are listed in Table 1. The crystallographic data for the structures of **1b**, **3a**, **2b**, and **3d** have been published as supplementary publication number 2016769(**1b**), 2016778(**3a**), 2016782(**2b**), and 2016780(**3d**) in the Cambridge Crystallographic Data Centre. A copy of these data can be obtained for free by applying to CCDC, 12 Union Road, Cambridge CB2 1EZ, UK, fax: 144-(0)1223-336033 or e-mail: deposit@ccdc.cam.ac.uk.

Table 1 Crystallographic data and structure refinement of **1b**, **2b**, **3a**, and **3d**.

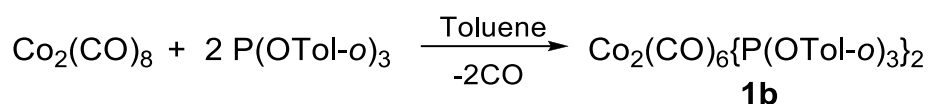
Compound	1b	2b	3a	3d
Empirical formula	C ₂₄ H ₂₁ CoO ₆ P	C ₃₇ H ₂₅ Co ₂ O ₈ P	C ₄₈ H ₃₆ Co ₂ O ₁₀ P ₂	C ₆₀ H ₅₂ Co ₂ O ₁₀ P ₂
Formula weight [g·mol ⁻¹]	495.315	746.40	952.57	1112.81
Temperature [K]	100(2)	100(2)	100(2)	100(2)
Crystal system	Monoclinic	Monoclinic	monoclinic	triclinic
Space group	<i>P</i> 2 ₁ / <i>c</i>	<i>P</i> 2 ₁ / <i>c</i>	<i>P</i> 2 ₁ / <i>c</i>	<i>P</i> -1
<i>a</i> [Å]	15.0006(5)	36.1532(13)	15.0759(9)	10.721(2)
<i>b</i> [Å]	10.8940(4)	10.0457(4)	9.0481(5)	13.699(3)
<i>c</i> [Å]	15.3868(4)	37.6940(15)	31.0989(19)	20.103(4)
α [°]	90	90	90	71.354(7)
β [°]	116.9430(10)	103.656(2)	95.597(2)	84.400(8)
γ [°]	90	90	90	70.183(6)
Volume [Å ³]	2241.53(13)	13302.9(9)	4221.9(4)	2631.6(9)
<i>Z</i>	4	16	4	2
ρ [g/cm ³]	1.468	1.491	1.499	1.404
μ [mm ⁻¹]	0.875	1.098	0.923	0.751

F(000)	1020.0	6080.0	1952.0	1152.0
Crystal size [mm ³]	0.261 × 0.252 × 0.092	0.562 × 0.232 × 0.142	0.719 × 0.037 × 0.015	0.194 × 0.129 × 0.066
Radiation	MoKα (λ = 0.71073)	MoKα (λ = 0.71073)	MoKα (λ = 0.71073)	MoKα (λ = 0.71073)
2Theta range for data collection θ [°]	5.306 to 64.492	4.204 to 61.052	5.43 to 55.998	4.36 to 63.02
Index ranges	−22 ≤ h ≤ 20, −16 ≤ k ≤ 15, −19 ≤ l ≤ 23	−51 ≤ h ≤ 51, −14 ≤ k ≤ 14, −53 ≤ l ≤ 49	−19 ≤ h ≤ 19, −11 ≤ k ≤ 11, −41 ≤ l ≤ 41	−14 ≤ h ≤ 15, −20 ≤ k ≤ 20, −29 ≤ l ≤ 29
Reflections collected	37160	221527	53184	98529
Independent reflections	7898 [<i>R</i> _{int} = 0.0379]	40638 [<i>R</i> _{int} = 0.0372]	10161 [<i>R</i> _{int} = 0.0559]	17501 [<i>R</i> _{int} = 0.0364]
Data/restraints/parameters	7898/0/414	40638/6/1740	10161/30/563	17501/46/785
Goodness-of-fit on F ²	1.051	1.040	1.076	1.027
Final <i>R</i> indexes [<i>I</i> > 2σ (<i>I</i>)]	<i>R</i> ₁ = 0.0464, <i>wR</i> ₂ = 0.1040	<i>R</i> ₁ = 0.0397, <i>wR</i> ₂ = 0.0863	<i>R</i> ₁ = 0.0417, <i>wR</i> ₂ = 0.0692	<i>R</i> ₁ = 0.0332, <i>wR</i> ₂ = 0.0746
Final <i>R</i> indexes (all data)	<i>R</i> ₁ = 0.0742, <i>wR</i> ₂ = 0.1270	<i>R</i> ₁ = 0.0601, <i>wR</i> ₂ = 0.0961	<i>R</i> ₁ = 0.0626, <i>wR</i> ₂ = 0.0752	<i>R</i> ₁ = 0.0450, <i>wR</i> ₂ = 0.0807
Largest diff. peak/hole [e Å ^{−3}]	0.86/−0.52	1.14/−0.83	0.46/−0.50	0.44/−0.40

3. Results and Discussion

3.1 Synthesis and Characterization of [Co₂(CO)₆{P(OTol-*o*)₃}₂] (**1b**)

The synthesis of dimer **1b** is similar to that of the previously reported P(OPh)₃ derivative, namely [Co₂(CO)₆{P(OPh)₃}₂] **1a**. On heating [Co₂(CO)₈] with 2.1 equivalents of tris(*o*-tolyl)phosphite in hot toluene at 90°C, the complex **1b** was isolated as a reddish-brown air-stable crystalline solid with a yield of 73% (Scheme 1).



Scheme 1 Preparation of bis(tris(*o*-tolyl)phosphite)hexacarbonyldicobalt complex **1b**

The D_{3h} symmetry of the complex was deduced from the IR spectrum exhibiting intense ν(CO) vibrations for the six carbonyls at 1957 cm^{−1} and a low-intensity peak at 1993 cm^{−1}. The magnetically equivalent phosphorus nuclei resulted in a broadened singlet resonating at δ 159.9 in the ³¹P NMR spectrum. The molecular structure of **1b** is in line with the solution data, as shown in

Figure 1. The symmetrically equivalent Co atoms adopt a trigonal pyramidal coordination sphere consisting of three equatorially oriented carbonyls, a metal-metal bond to the adjacent $\text{Co}(\text{CO})_3\text{P}$ moiety, and a Co-bound phosphite ligand. The length of the Co-Co bond (2.6688(5) Å) is quite comparable to that of $[\text{Co}_2(\text{CO})_6\{\text{P}(\text{OPh})_3\}_2]$ (2.6722(4) Å), but remarkably shorter than that of $[\text{Co}_2(\text{CO})_6\{\text{P}(\text{O}-2,4\text{-}t\text{-Bu}_2\text{C}_6\text{H}_3)_3\}_2]$ bearing two bulky (2,4-tert-butylphenyl)phosphite ligands (2.706(5) Å) [28, 29]. For comparison, the Co-Co distance reported for $[\text{Co}_2(\text{CO})_6\{\text{P}(\text{OiPr})_3\}_2]$ was 2.6544(12) Å, reflecting the steric and electronic impacts of the OR substituents on the metal-metal separation [25]. It is noted that the Co-Co bond length of $[\text{Co}_2(\text{CO})_8]$ itself shrinks to a value of 2.522(1) Å [40, 41]. The Co-P distances in the nearly *trans*-oriented $\text{P}(\text{OAr})_3$ ligands (175.33(3)°) of **1b** were close to those reported for **1a** (2.1218(6) vs. 2.1224(4) Å).

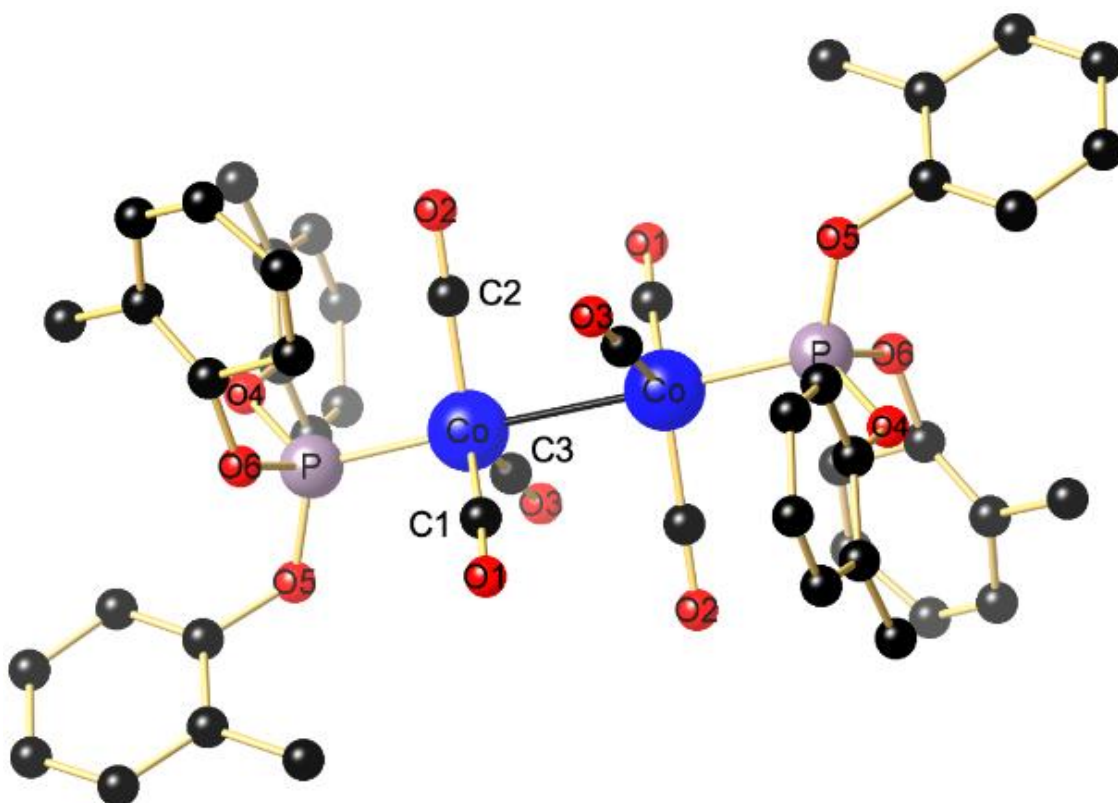
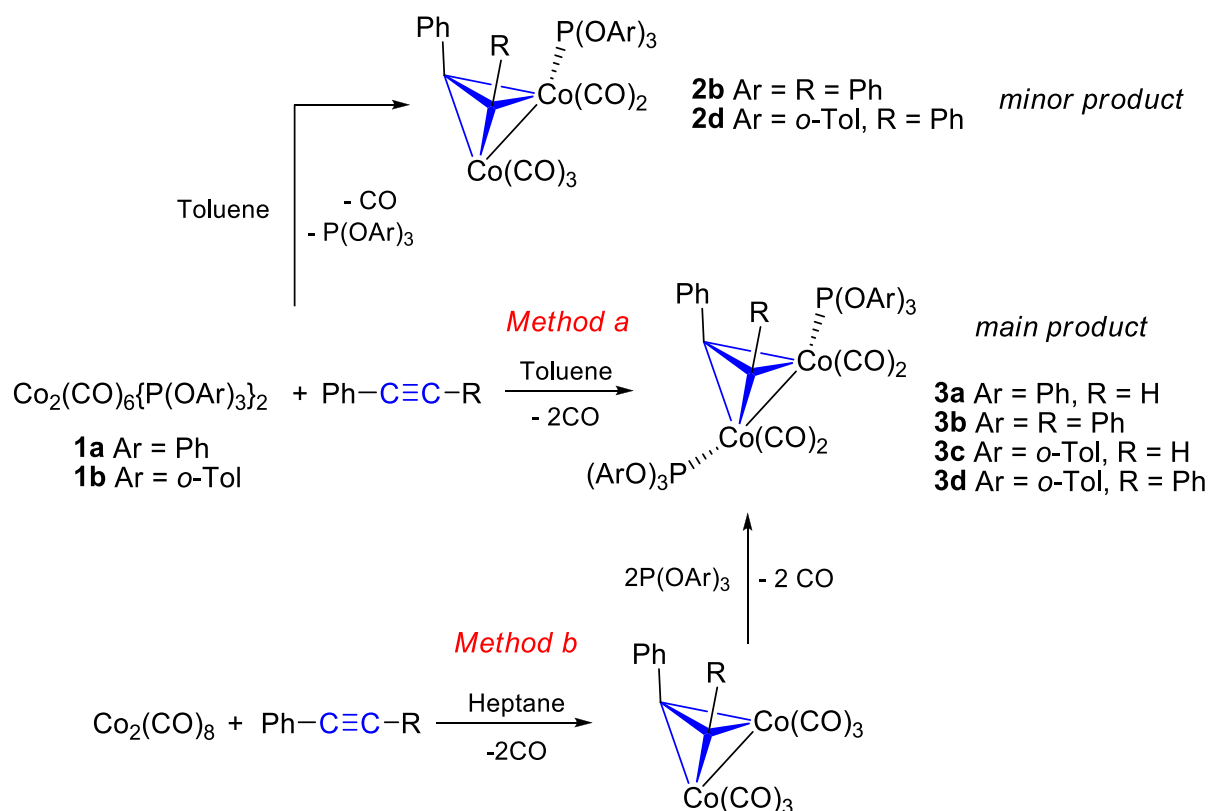


Figure 1 Molecular structure of $[\text{Co}_2(\text{CO})_6\{\text{P}(\text{OTol-}o)_3\}_2]$ (**1b**). The H atoms are omitted for clarity. Selected bond lengths [Å] and angles [°]: Co-Co 2.6688(5), Co-P 2.1218(6), Co-C1 1.777(2), Co-C2 1.795(2), Co-C3 1.795(2), P-Co-Co 175.33(3), C1-Co-P 91.32(8), C1-Co-C2 122.48(12), C1-Co-C3 116.26(11), C2-Co-P 95.40(7), C3-Co-P 98.21(7). A thermal ellipsoid plot of **1b** at the probability level of 50% is shown in Figure S16 of the Supporting Information.

3.2 Synthesis and Characterization of Dimetallatetrahedranes $\{(\text{ArO})_3\text{P}\}(\text{OC})_2\text{Co-Co}(\mu\text{-PhC}\equiv\text{CR})(\text{CO})_2\{\text{P}(\text{OAr})_3\}$

The reaction of equimolar quantities of $[\text{Co}_2(\text{CO})_6\{\text{P}(\text{OAr})_3\}_2]$ and $\text{PhC}\equiv\text{CR}$ in hot toluene was monitored by IR spectroscopy until the disappearance of the carbonyl bands of the initial phosphite cobalt complex, indicating the formation of dimetallatetrahedrane complexes. Alternatively, these compounds were isolated after a two-step sequence involving the acetylene

complexation of the dicobaltoctacarbonyl complex, followed by the substitution of two CO groups by the aryl phosphite ligands (Scheme 2). The IR monitoring indicated the formation of minor amounts of a monosubstituted phosphite compound characterized by the carbonyl stretch at *ca.* 2065 cm⁻¹ [22]. The crystallization of the reaction mixture in toluene or heptane afforded **3a-d** as dark red stable solids in high yields (near 85%). The reaction of diphenylacetylene with [Co₂(CO)₆{P(OAr)₃}₂] leads to small amounts of monosubstituted derivatives [Co₂(CO)₆{(ArO)₃P}(OC)₂Co-Co(μ-PhC≡CPh)(CO)₃]. The compounds **2b** (Ar = Ph) and **2d** (Ar = *o*-Tol) were isolated as black crystals and brown powder, respectively. Thus, it was presumed that the coordination of the alkyne implies the first-step elimination of carbonyl and phosphite groups in this side reaction, leading to the formation of monophosphite tetrahedrane. The latter reacts with the *in situ* liberated phosphate, causing the substitution of a second carbonyl ligand (Scheme 2). Another possible mechanistic pathway initially implies the formation of bisphosphite tetrahedrane **3**, followed by the partial dissociation of a phosphite ligand. Further mechanistic studies using the other P(OR)₃ ligands should be performed to clarify this point. All the complexes described therein were characterized by IR and NMR spectroscopy.



Scheme 2 Synthesis of (arylphosphite)dicobalt tetrahedrane complexes

The IR (ATR) spectra of [Co₂(CO)₆{(ArO)₃P}(OC)₂Co-Co(μ-PhC≡CR)(CO)₂{P(OAr)₃}] displayed similar two strong absorptions at about 2030 and 1980 cm⁻¹. Another weak CO vibration appeared near 1950 cm⁻¹ as a shoulder-type peak. The representative spectrum of compound **3d** is illustrated in Figure 2. This IR spectroscopic observation in the solid state was in agreement with the structural characterization of compounds **3a** and **3d** (see below). In solution, four bands in the CO stretching region were generally observed for the diaxially phosphane-substituted tetrahedrane complexes

such as $[(\text{Ph}_3\text{P})(\text{OC})_2\text{Co}-\text{Co}(\mu\text{-PhC}\equiv\text{CPh})(\text{CO})_2(\text{PPh})_3]$ [22]. This characteristic pattern was observed in the IR spectra of the complexes in cyclohexane, and the corresponding wavenumbers are given in the experimental part. In the lower-symmetry monophosphite complexes **2b** and **2d**, the five $\nu(\text{CO})$ bands appeared in the terminal carbonyl region (Figure 2). The IR spectra matched with those reported by Manning *et al.* for $[\{(\text{MeO})_3\text{P}\}(\text{OC})_2\text{Co}-\text{Co}(\mu\text{-PhC}\equiv\text{CPh})(\text{CO})_3]$ and $[(\text{Ph}_3\text{P})(\text{OC})_2\text{Co}-\text{Co}(\mu\text{-PhC}\equiv\text{CPh})(\text{CO})_3]$, which discussed the substitution of an axial carbonyl ligand by the P-donor ligand, regardless of the cone angle [22].

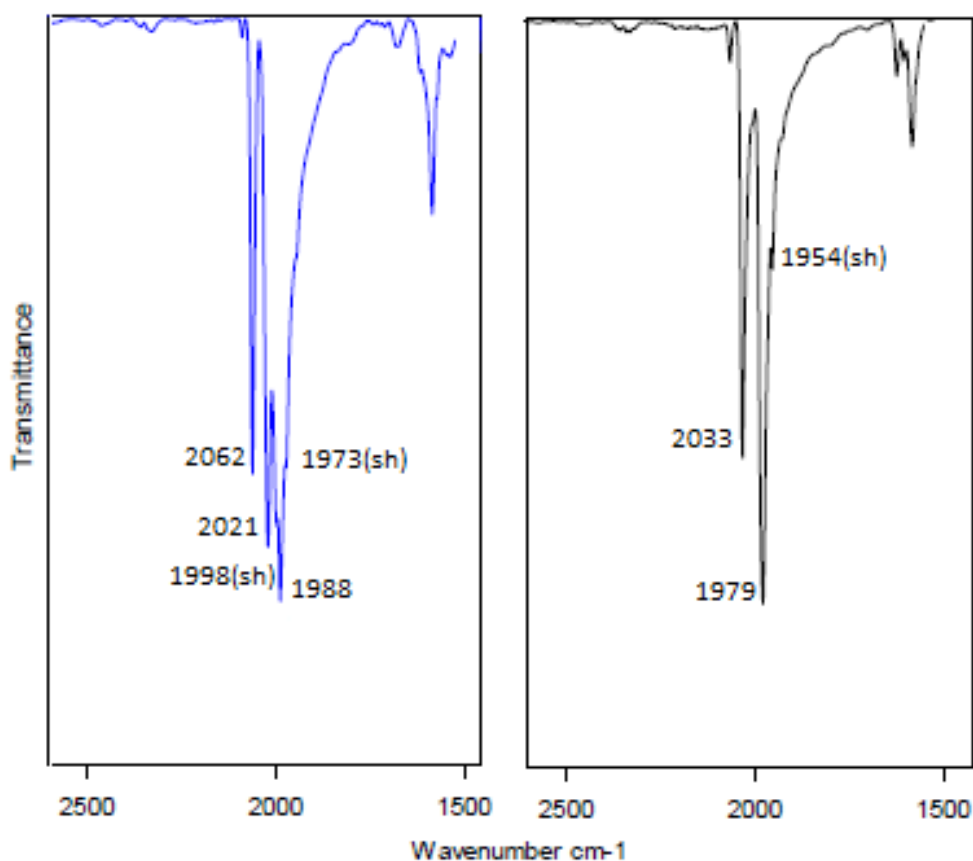


Figure 2 IR (ATR) spectra of diphenylacetylene $\text{P}(\text{OTol-}o)_3$ -dicobalt derivatives **2d** (left) and **3d** (right) in the $\nu(\text{CO})$ region.

The NMR data are reported in the experimental part. The ^1H NMR spectra show a line-broadening of all the peaks probably due to the quadrupolar relaxation of the ^{59}Co nuclei [20]. The acetylenic proton of $[\text{Co}_2(\mu\text{-PhC}\equiv\text{CH})(\text{CO})_6]$ was reported to resonate at δ 6.38 [12], while those of the phenylacetylene derivatives **3a** and **3b** were shifted towards high-field as a broad signal (due to unresolved 3J P-H coupling) near 5 ppm. Compared to free phenylacetylene (δ 3.06), the downfield shift of the terminal proton is in agreement with the reduction of the triple bond character after complexation. The observation of a single ^{31}P NMR resonance peak for **3a-d** is consistent with the magnetically equivalent phosphorus nuclei in the disubstituted compounds. The chemical shifts were quite affected by the nature of the coordinated alkyne. An upfield shift of *ca.* 7 ppm was observed for the diphenylacetylene derivatives compared to that of the phenylacetylene derivatives. The ^{31}P NMR spectroscopy showed no differentiation between the mono- and disubstituted complexes due to the presence of singlet resonance peak of identical

chemical shifts in both cases. However, the ^{13}C NMR spectra of the complexes were significantly different in the carbonyl region (Figure 3). In the disubstituted complexes **3a-d**, a single resonance was observed for the carbonyls around 200 ppm, while two distinct broad singlets were observed for the terminal carbonyls in $[\{(\text{ArO})_3\text{P}\}(\text{OC})_2\text{Co-Co}(\mu\text{-PhC}\equiv\text{CPh})(\text{CO})_3]$ (Ar = Ph, **2b**; Ar = *o*-Tol, **2d**). Besides, a downfield shift of about 3 ppm was observed for the acetylenic carbon atoms (Figure 3).

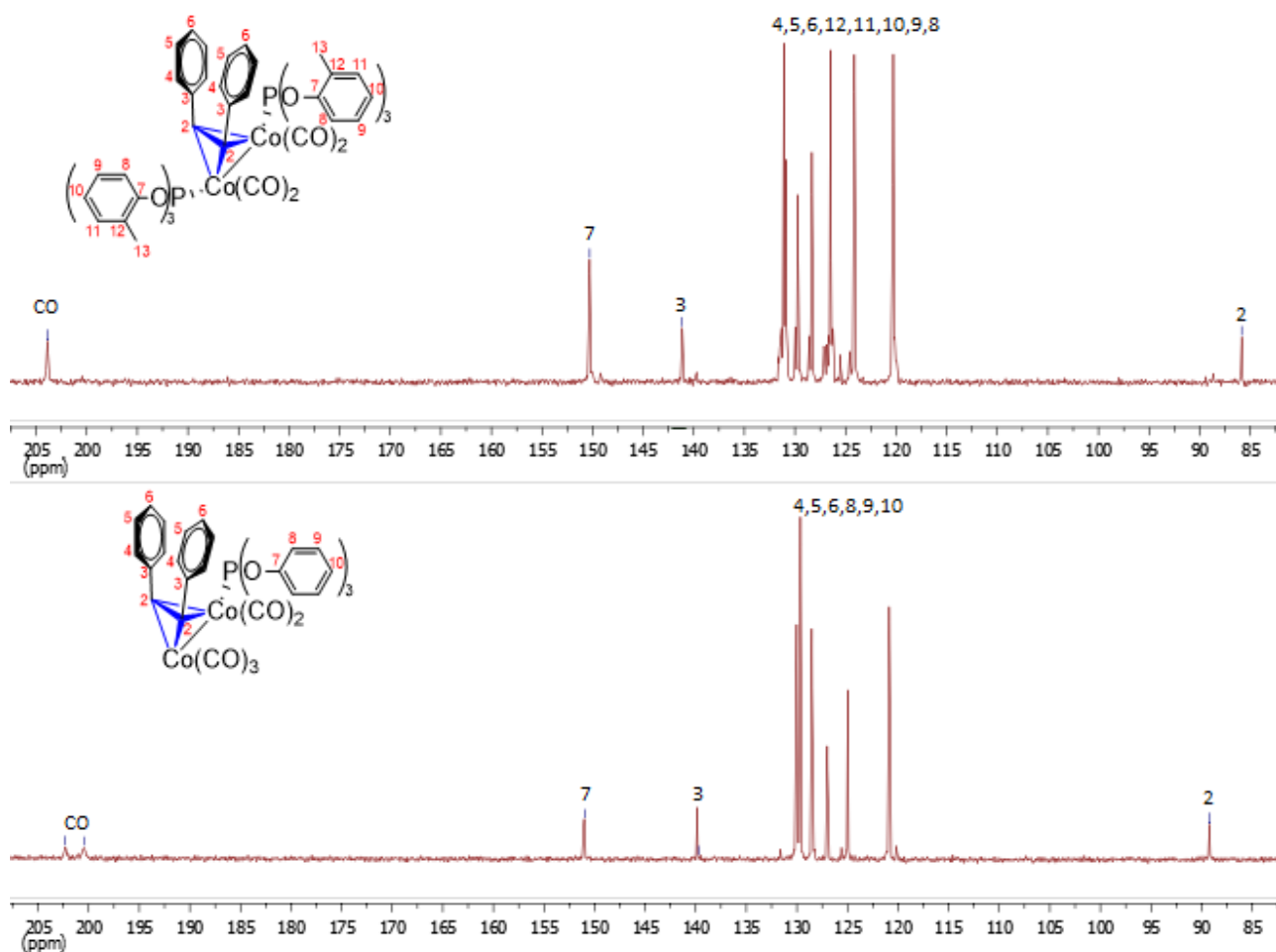


Figure 3 $^{13}\text{C}\{^1\text{H}\}$ NMR spectra of **2b** (bottom) and **3d** (top) in the range of 80–210 ppm recorded in CDCl_3 .

The molecular structure for the dicobalttetrahedrane scaffold of **3a** is shown in Figure 4. The $\text{PhC}\equiv\text{CH}$ moiety was nearly orthogonally oriented with respect to the vector of the Co–Co bond ($89.436(16)^\circ$). The two crystallographically non-equivalent $\text{P}(\text{OPh})_3$ ligands lost their ideal linear *trans*-disposition of 180° observed in the precursor $[\text{Co}_2(\text{CO})_6\{\text{P}(\text{OPh})_3\}_2]$ **1a** complex with the P1–Co1–Co2–P2 dihedral angle of 11.96° . In contrast, the mean Co–P distance of **3a** was close to that of the precursor **1a** complex ($2.1303(7)$ vs. $2.1224(4)$ Å). There are no crystallographic data for the parent compound $[\text{Co}_2(\mu\text{-PhC}\equiv\text{CH})(\text{CO})_6]$. However, several entries were reported in the CSD base for the phosphane-ligated phenylacetylene dicobalttetrahedranes, as listed in Table 2. Generally, the Co–Co bond distances lie in the range of $2.4287(8)$ to $2.5140(5)$ Å. However, the Co–Co bond distance of **3a** was observed in the mid-range with a value of $2.4665(6)$ Å.

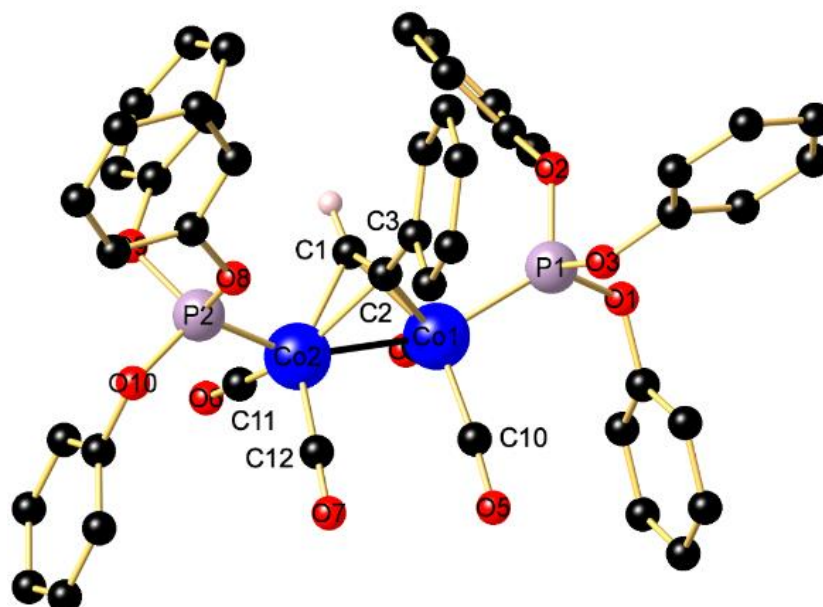
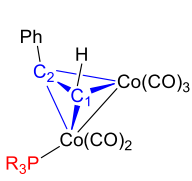
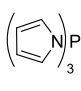
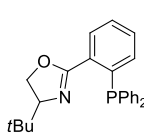
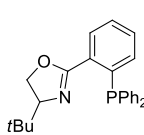
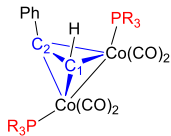
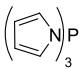
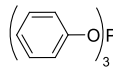
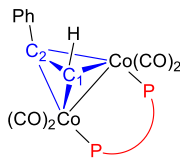
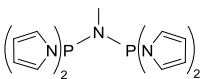
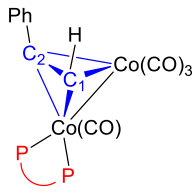


Figure 4 Molecular structure of **3a**. All the H atoms apart from the acetylenic ones are omitted for clarity. The C-bound hydrogen atom on C1 was located in the difference Fourier map, and refined independently. Selected bond lengths [Å] and angles [°]: Co1-Co2 2.4666(5), Co1-P1 2.1292(7), Co2-P2 2.1313(7), Co1-C1 1.951(2), Co1-C2 1.994(2), Co2-C1 1.970(2), Co2-C2 1.970(2), Co1-C9 1.795(2), Co1-C10 1.794(3), Co2-C11 1.798(2), Co2-C12 1.797(2), C1-C2 1.337(3), P1-Co1-Co2 147.52(2), P2-Co2-Co1 150.93(2), P1-Co1-C1 105.06(7), P1-Co1-C2 96.45(7), P2-Co2-C1 105.08(7), P2-Co2-C2 99.54(7), P1-Co1-C10 100.50(8), P1-Co1-C9 99.34(8), P2-Co2-C11 101.70(8), P2-Co2-C12 94.19(8), Co2-C1-Co1 77.96(9), Co2-C2-Co1 76.97(8), C1-C2-C3 140.3(2). The thermal ellipsoid plot of **3a** at the probability level of 50% is shown in Figure S17 of the Supporting Information.

Table 2 Relevant bond lengths (Å) in crystallographically characterized phosphane- or diarsane-substituted tetrahedrane scaffolds featuring a μ -PhCCH-Co₂ fragment.

Complex	Phosphine ligand	Co-Co	C ₁ -C ₂	Co ₁ C ₁ ; Co ₁ C ₂ Co ₂ C ₁ ; Co ₂ C ₂	CSD reference
		2.483(1)	1.344(9)	1.956(8), 1.988(7), 1.960(7), 1.979(6)	MAZBUK [42]
		2.480(1)	1.351(9)	1.950(7), 2.001(6), 1.991(7), 1.986(6), 1.981(6),	
		2.468(3)	1.326(9)	1.993(6), 1.945(6), 1.948(6)	NAQHIW [43]

		2.509(1)	1.332(4)	1.961(4), 1.979(4), 1.950(4), 1.987(4), 1.951(3), 1.994(2), 1.970(3), 1.969(2)	MAZCAR [42]
		2.4665(6)	1.337(3)	1.954(5), 1.967(4), 1.955(5), 1.940(4), 1.943(2), 1.968(2), 1.955(2), 1.956(2), 1.948(4), 1.963(4), 1.950(3), 1.954(3), 1.960(3), 1.974(3), 1.958(4), 1.965(3), 1.936(3), 1.950(4), 1.931(3), 1.966(3), 1.950(6), 1.923(6), 1.953(5), 1.968(7)	This work
	$\text{Ph}_2\text{P}-\text{CH}_2-\text{PPh}_2$	2.4776(7)	1.340(7)		MEEJJOA [44]
	$\text{Ph}_2\text{P}-\text{N}(\text{CH}_3)-\text{PPh}_2$	2.445(1)	1.327(3)		MEJJUG [44]
	$\text{F}_2\text{P}-\text{N}(\text{CH}_3)-\text{PF}_2$	2.4396(8)	1.331(5)		MEJKAN [44]
	$\{(\text{F}_3\text{C})_2\text{HCO}\}_2\text{P}-\text{N}(\text{CH}_3)-\text{P}\{\text{OCH}(\text{CF}_3)_2\}_2$	2.4435(8)	1.321(3)		MEJKER [44]
		2.4287(8)	1.320(4)		MEJKIV [44]
	$\text{Ph}_2\text{As}-\text{O}-\text{AsPh}_2$	2.484(1)	1.341(9)		WOMPET [45]
	$(\text{H}_3\text{C})(\text{tBu})\text{P}(\text{N}(\text{C}_6\text{H}_4))_2$	2.5140(5)	1.338(4)	1.921(3), 1.933(3), 2.010(3), 1.981(3), 1.920(8), 1.929(7), 1.991(9), 1.983(8)	GASPIC [46]
	$\text{Ph}_2\text{P}-\text{CH}=\text{CH}-\text{PPh}_2$	2.495(2)	1.31(1)		VAHGAN [47]

According to Scheme 2, the compounds **1a** and **1b** were treated with diphenylacetylene $\text{PhC}\equiv\text{CPh}$ to study the impact of an internal alkyne on the structural features. Although the targeted bis(phosphite) complexes **3b** and **3d** were readily isolated, the presence of another minor species featuring an $\nu(\text{CO})$ stretch at about 2060 cm^{-1} was observed by IR monitoring attributing to the $\{[(\text{PhO})_3\text{P}]\{\text{OC}\}_2\text{Co}-\text{Co}(\mu\text{-PhC}\equiv\text{CPh})(\text{CO})_3\}$ complex (**2b**). As mentioned above, the monophosphite complex **2b** was successfully isolated by fractional crystallization, allowing

complete spectroscopic characterization. The complete characterization of **2b** crystallizing in the monoclinic space group $P2_1/c$ was performed by the X-ray diffraction study. It is noted that the corresponding unit cell is composed of four independent molecules. The following values used in the structural discussion are related to the unit presented in Figure 5. The dicobaltatetrahedrane scaffold bears the $P(OPh)_3$ ligand at the axial position of the $Co1(CO)_2$ moiety. The Co-P bond length was slightly elongated with respect to that of the $[Co_2(CO)_6\{P(OPh)_3\}_2]$ **1a** complex (2.1404(5) vs. 2.1224(4) Å). The comparison of the resultant complex with the parent compound $[(OC)_3Co-Co(\mu-PhC\equiv CPh)(CO)_3]$ revealed that the Co-Co bond length is (within the experimental error) not affected by the substitution of a carbonyl group by $P(OPh)_3$ (2.4760(4) vs. 2.476(2) Å) [48]. The mean Co- $\mu(C)$ bond distance of 1.9679(18) was in agreement with that reported for $[(OC)_3Co-Co(\mu-PhC\equiv CPh)(CO)_3]$ (1.97(1) Å). The consistency was observed in the C=C bond length values (1.351(3) vs. 1.36(1) Å) of the complex and bridging diphenylacetylene unit as well. Table 3 gives the relevant bond lengths of the previously reported phosphane-substituted dicobaltatetrahedrane scaffolds bridged by $PhC\equiv CPh$.

The molecular structure of the dicobaltatetrahedrane **3d** complex is shown in Figure 6. There were no significant variations in the bond lengths and angles relative to similar compounds.

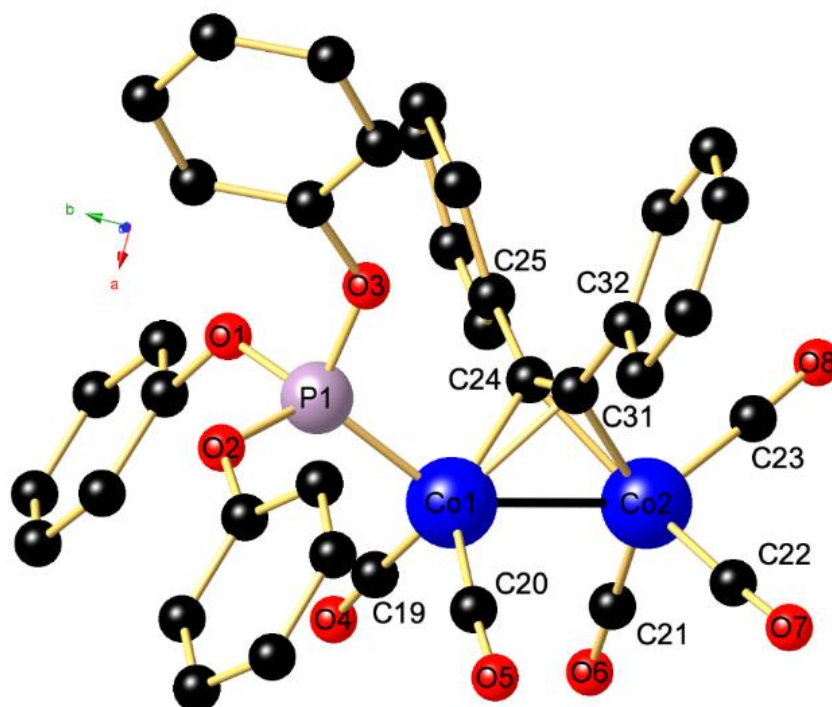
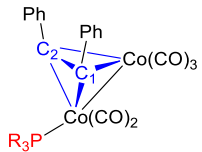
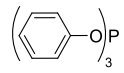
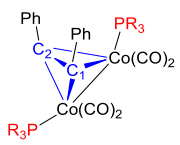
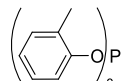
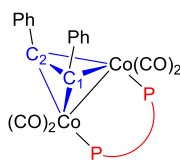
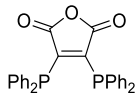
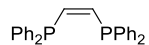
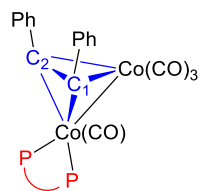


Figure 5 Molecular structure of $[(PhO)_3P\{OC\}_2Co-Co(\mu-PhC\equiv CPh)(CO)_3]$ (**2b**). The H atoms are omitted for clarity. Only one of the four independent molecules in the unit cell is shown. Selected bond lengths [Å] and angles [°]: Co1-Co2 2.4760(4), Co1-P1 2.1404(5), Co1-C19 1.809(2), Co1-C20 1.808(2), Co1-C24 1.9608(18), Co1-C31 1.9533(18), Co2-C21 1.817(2), Co2-C22 1.812(2), Co2-C23 1.795(2), Co2-C24 1.9704(18), Co2-C31 1.9871(18), C24-C31 1.351(3); P1-Co1-Co2 145.494(18), P1-Co1-C24 96.83(6), P1-Co1-C31 96.56(), P1-Co1-C19 100.60(6), P1-Co1-C20 102.75(7), Co1-C24-Co2 78.08(7), Co1-C31-Co2 77.85(6), C25-C24-C31 143.91(13), C24-C31-C32 143.11(17). The thermal ellipsoid plot of **2b** at the probability level of 50% is shown in Figure S18 of the Supporting Information.

Table 3 Relevant bond lengths (Å) in crystallographically characterized phosphane-substituted tetrahedrane scaffolds featuring a μ -PhCCPh-Co₂ fragment.

Complex	Phosphine ligand	Co-Co	C ₁ -C ₂	Co ₁ C ₁ ; Co ₁ C ₂ Co ₂ C ₁ ; Co ₂ C ₂	CSD reference
		2.4760(4)	1.351(3)	1.9608(18), 1.9533(18) 1.9704(18), 1.9871(18)	This work
		2.4548(4)	1.349(2)	1.9583(18), 1.9628(18) 1.9893(18), 1.9832(19)	
		2.4595(4)	1.346(3)	1.9653(19), 1.9461(19) 1.976(2), 1.9966(19)	
		2.4718(4)	1.349(3)	1.9578(18), 1.9494(18) 1.9707(18), 1.9918(18)	
		2.4642	1.3461(17)	1.9937(13), 1.9618(13) 1.9593(14), 1.9953(13)	This work
		2.459(2)	1.33(1)	1.97(1), 1.95(1) 1.92(1), 1.94(1)	TDAMCO [49]
		2.469(4)	1.29(3)	1.91(2), 2.01(2) 1.91(2), 1.93(2)	



2.485(2)

1.31(2)

1.930(9), 1.92(1)
1.99(1), 1.98(1)

POMSIT [50]

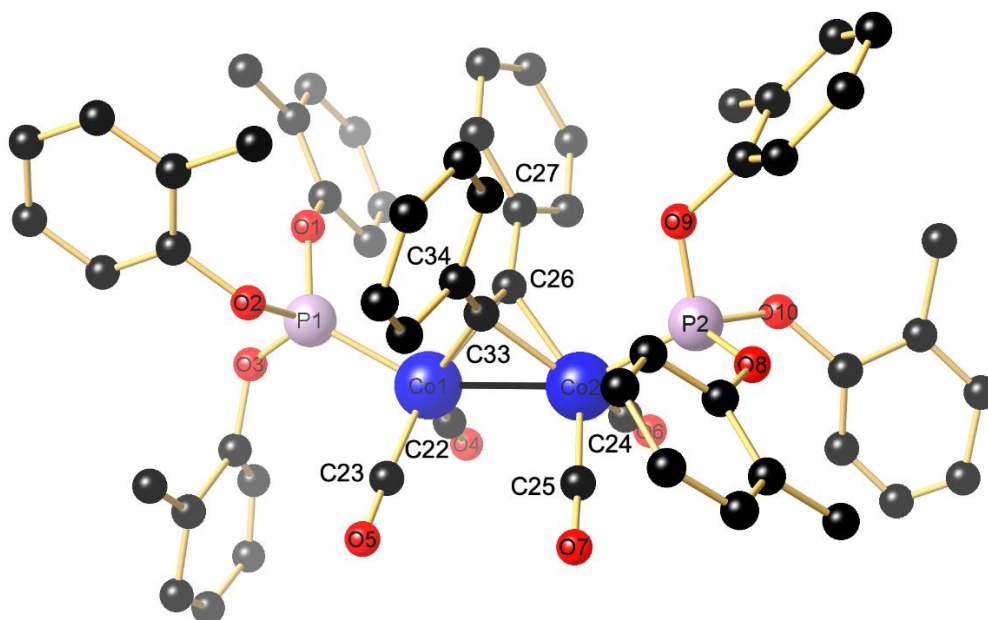


Figure 6 Molecular structure of $[\{(o\text{-TolO})_3\text{P}\}(\text{OC})_2\text{Co}-\text{Co}(\mu\text{-PhC}\equiv\text{CPh})(\text{CO})_2\{\text{P}(\text{OTol-}o)_3\}]$. (**3d**). The H atoms are omitted for clarity. Selected bond lengths [Å] and angles [°]: Co1-Co2 2.4642(5), Co1-P1 2.1525(5), Co1-P2 2.1447(6), Co1-C22 1.7961(14), Co1-C23 1.8035(14), Co1-C26 1.9937(13), Co1-C33 1.9953(13), Co2-C24 1.7991(14), Co2-C25 1.8036(14), Co2-C26 1.9593(13), Co2-C33 1.9953(13), C24-C31 1.3461(17); P1-Co1-Co2 151.652(13), P1-Co1-C22 98.43(5), P1-Co1-C23 99.32(5), P1-Co1-C26 101.86(4), P1-Co1-C33 103.26(4), Co1-C26-Co2 77.12(5), Co1-C33-Co2 77.03(4), C27-C26-C34 141.64(12), C26-C33-C34 142.23(112), P2-Co2-Co1 151.923(14), P2-Co2-C24 97.25(5), P2-Co2-C25 98.84(4), P2-Co2-C26 101.67(6), P2-Co2-C33 103.61(4). The thermal ellipsoid plot of **3d** at the probability level of 50% is shown in Figure S19 of the Supporting Information.

4. Conclusions

In this study, the structural analyses of four dicobalt compounds were performed to crystallographically characterize the arylphosphite-substituted dicobalt complexes. Besides, the conversion of $[\{\text{Co}_2(\text{CO})_6\{\text{P}(\text{OAr})_3\}_2}]$ to dicobaltatetrahedranes is accompanied by the partial dissociation of one of the $\text{P}(\text{OAr})_3$ ligands, leading to the formation of $[\{(\text{ArO})_3\text{P}\}(\text{OC})_2\text{Co}-\text{Co}(\mu\text{-PhC}\equiv\text{CPh})(\text{CO})_3]$ as a minor component. The current studies are focused on phosphite-substituted dicobaltatetrahedranes bearing functionalized *N*-heterocyclic alkynes, intending to utilize these complexes as substrates for the Pauson-Khand reactions and use thioether-functionalized compounds $[\{(\text{R}'\text{O})_3\text{P}\}(\text{OC})_2\text{Co}-\text{Co}(\mu\text{-RSCH}_2\text{C}\equiv\text{CCH}_2\text{SR})(\text{CO})_2\{\text{P}(\text{OR}')_3\}]$ as precursors for the development of polynuclear heterometallic assemblies by the coordination of other metal fragments to the *S*-donor sites of the alkyne.

Acknowledgments

We thank Stephanie Boullanger for recording the NMR spectra.

Additional Materials

The following additional materials are uploaded at the page of this paper.

1. Figure S1: IR(ATR) spectrum of $\text{Co}_2(\text{CO})_6\{\text{P}(\text{OTol-}o)_3\}_2$ (**1b**).
2. Figure S2: $^{31}\text{P}\{^1\text{H}\}$ NMR spectrum of $\text{Co}_2(\text{CO})_6\{\text{P}(\text{OTol-}o)_3\}_2$ (**1b**) recorded in CDCl_3 .
3. Figure S3: $^{13}\text{C}\{^1\text{H}\}$ NMR spectrum of $\text{Co}_2(\text{CO})_6\{\text{P}(\text{OTol-}o)_3\}_2$ (**1b**) recorded in CDCl_3 .
4. Figure S4: IR(ATR) spectrum of $\text{Co}_2(\text{CO})_4\{\text{P}(\text{OPh})_3\}_2(\mu\text{-PhCCH})$ (**3a**).
5. Figure S5: $^{31}\text{P}\{^1\text{H}\}$ NMR spectrum of $\text{Co}_2(\text{CO})_4\{\text{P}(\text{OPh})_3\}_2(\mu\text{-PhCCH})$ (**3a**) recorded in CDCl_3 .
6. Figure S6: IR(ATR) spectrum of $\text{Co}_2(\text{CO})_4\{\text{P}(\text{OTol-}o)_3\}_2(\mu\text{-PhCCH})$ (**3b**).
7. Figure S7: $^{31}\text{P}\{^1\text{H}\}$ NMR spectrum of $\text{Co}_2(\text{CO})_4\{\text{P}(\text{OTol-}o)_3\}_2(\mu\text{-PhCCH})$ (**3b**) recorded in CDCl_3 .
8. Figure S8: IR(ATR) spectrum of $\text{Co}_2(\text{CO})_4\{\text{P}(\text{OPh})_3\}_2(\mu\text{-PhCCPh})$ (**3c**).
9. Figure S9: $^{31}\text{P}\{^1\text{H}\}$ NMR spectrum of $\text{Co}_2(\text{CO})_4\{\text{P}(\text{OPh})_3\}_2(\mu\text{-PhCCPh})$ (**3c**) recorded in CDCl_3 .
10. Figure S10: IR(ATR) spectrum of $\text{Co}_2(\text{CO})_5\{\text{P}(\text{OPh})_3\}(\mu\text{-PhCCPh})$ (**2b**).
11. Figure S11: $^{31}\text{P}\{^1\text{H}\}$ NMR spectrum of $\text{Co}_2(\text{CO})_5\{\text{P}(\text{OPh})_3\}(\mu\text{-PhCCPh})$ (**2b**) recorded in CDCl_3 .
12. Figure S12: IR(ATR) spectrum of $\text{Co}_2(\text{CO})_4\{\text{P}(\text{OTol-}o)_3\}_2(\mu\text{-PhCCPh})$ (**3d**).
13. Figure S13: $^{31}\text{P}\{^1\text{H}\}$ NMR spectrum of $\text{Co}_2(\text{CO})_4\{\text{P}(\text{OTol-}o)_3\}_2(\mu\text{-PhCCPh})$ (**3d**) recorded in CDCl_3 .
14. Figure S14: IR(ATR) spectrum of $\text{Co}_2(\text{CO})_5\{\text{P}(\text{OTol-}o)_3\}(\mu\text{-PhCCPh})$ (**2d**).
15. Figure S15: $^{31}\text{P}\{^1\text{H}\}$ NMR spectrum of $\text{Co}_2(\text{CO})_5\{\text{P}(\text{OTol-}o)_3\}(\mu\text{-PhCCPh})$ (**2d**) recorded in CDCl_3 .
16. Figure S16: A thermal ellipsoid plot of **1b** at the 50% probability level.
17. Figure S17: A thermal ellipsoid plot of **3a** at the 50% probability level.
18. Figure S18: A thermal ellipsoid plot of **2b** at the 50% probability level.
19. Figure S19: A thermal ellipsoid plot of **3d** at the 50% probability level.

Author Contributions

I. Jourdain and M. Knorr performed the synthetic work and wrote the manuscript, L. Brieger and C. Strohmam determined the crystal structures.

Funding

We are grateful to the Université de Franche-Comté for financial support via a Chrysalide funding .

Competing Interests

The authors have declared that no competing interests exist.

References

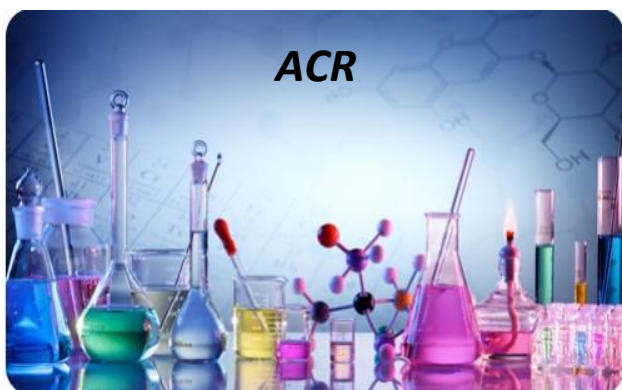
1. Greenfield H, Sternberg HW, Friedel RA, Wotiz JH, Markby R, Wender I. Acetylenic dicobalt hexacarbonyls. Organometallic compounds derived from alkynes and dicobalt octacarbonyl. J Am Chem Soc. 1956; 78: 120-124.
2. Sly WG. The Molecular configuration of dicobalt hexacarbonyl diphenylacetylene. J Am Chem Soc. 1959; 81: 18-20.

- Atwood JD. *Comprehensive Organometallic Chemistry II, Vol 8: Cobalt, Rhodium and Iridium*. California: Elsevier; 2002.
- Lockwood RF, Nicholas KM. Transition metal-stabilized carbenium ions as synthetic intermediates. I. α -[(alkynyl)dicobalt hexacarbonyl] carbenium ions as propargylating agents. *Tetrahedron Lett.* 1977; 18: 4163-4165.
- El-Amouri H, Gruselle M, Jaouen G, Daran JC, Vaissermann J. Synthesis, structure and reactivity of a novel series of propargylic cationic derivatives: $[\text{Co}_2(\text{CO})_6(\text{CH}\equiv\text{CCH}_2\text{SR}_1\text{R}_2)]\text{BF}_4$, $[(\text{Co}_2(\text{CO})_6(\text{CH}\equiv\text{CCH}_2\text{PR}_3))\text{BF}_4$ and $[\text{Co}_2(\text{CO})_6(\text{CH}\equiv\text{CCH}_2\text{Py})]\text{BF}_4$. *Inorg Chem.* 1990; 29: 3238-3242.
- Went MJ. Synthesis and reactions of polynuclear cobalt-alkyne complexes. *Inorg Chem.* 1997; 41: 69-126.
- Moore A, Ostermann J, Müller-Bunz H, Ortin Y, McGlinchey MJ. Metal-stabilized carbocations derived from monoterpenes: Dicobalt hexacarbonyl complexes of alkynyl-terpenols. *Tetrahedron.* 2016; 72: 4186-4193.
- Nicholas KM. Chemistry and synthetic utility of cobalt-complexed propargyl cations. *Acc Chem Res.* 1987; 20: 207-214.
- Pauson PL, Khand IU. Uses of cobalt-carbonyl acetylene complexes in organic synthesis. *Ann NY Acad Sci.* 1977; 295: 2-14.
- Devasagayaram A, Periasamy M. A simple convenient synthesis of alkyne-dicobalt hexacarbonyl complexes and their utilization in the Pauson-Khand cyclopentenone synthesis. *Tetrahedron Lett.* 1989; 30: 595-6.
- Verdaguer X, Moyano A, Pericrıs MA, Riera A, Greene AE, Piniella JF et al. Camphor-derived alcohols as chiral auxiliaries for asymmetric Pauson-Khand bicyclizations. Enantioselective synthesis of α -methoxyenones. *J Organomet Chem.* 1992; 433: 305-310.
- Hay AM, Kerr WJ, Kirk GG, Middlemiss D. Highly efficient enantioselective Pauson-Khand reactions. *Organometallics.* 1995; 14: 4986-4988.
- Derdau V, Laschat S, Dix I, Jones PG. Cobalt-Alkyne complexes with diphosphine ligands as mechanistic probes for the Pauson-Khand reaction. *Organometallics.* 1999; 18: 3859-3864.
- Gibson SE, Stevenazzi A. The Pauson-Khand reaction: The catalytic age is here! *Angew Chem Int Ed.* 2003; 42: 1800-1810.
- Blanco-Urgoiti J, Añorbe L, Pérez-Serrano L, Domínguez G, Pérez-Castells J. The Pauson-Khand reaction, a powerful synthetic tool for the synthesis of complex molecules. *Chem Soc Rev.* 2004; 33: 32-42.
- Werner H. Peter Ludwig Pauson (1925–2013). *Angew Chem Int Ed.* 2014; 53: 3309-3309.
- Elliot DJ, Holah DG, Hughes AN, Magnuson VR, Moser IM. Synthesis, reactions, and X-Ray crystal-structures of $\text{Co}_2(\mu\text{-Ph}_2\text{PCH}_2\text{PPh}_2)_2(\text{CO})_4$ and $\text{Co}_2(\mu\text{-Ph}_2\text{PCH}_2\text{PPh}_2)_2(\mu\text{-CO})_2(\text{CO})_2$. *Bull Soc Chim Fr.* 1992; 676-685.
- Pohl D, Ellermann J, Knoch FA, Moll M, Bauer W. Chemie polyfunktioneller Moleküle CXIII. Komplexe des Dicobaltcarbonyls mit den Liganden Bis(diphenylphosphino)amin und -amid. *J Organomet Chem.* 1994; 481: 259-274.
- Hong FE, Huang YL, Chen HL. Observations on reaction pathways of dicobalt octacarbonyl with alkynyl amines. *J Organomet Chem.* 2004; 689: 3449-3460.
- Saito T, Sawada S. ^{59}Co quadrupole effects on the ^1H , ^{31}P and ^{59}Co NMR spectra of $\text{HFeCo}_3(\text{CO})_9[\text{P}(\text{OCH}_3)_3]_3$ and the ^1H NMR spectra of other derivatives. *Bull Chem Soc Jap.* 1985; 58: 459-463.

21. Szabo P, Fekete L, Bor G, Nagy-Magos Z, Marko L. Phosphorus-containing cobalt carbonyls. III. Monosubstituted derivatives of diobalt octacarbonyl with phosphines and phosphites. *J Organomet Chem.* 1968; 12: 245-248.
22. Chia LS, Cullen WR, Franklin M, Manning AR. Reactions of $(RC\equiv CR')Co_2(CO)_6$ complexes with mono- and bidentate Group 5 ligands. *Inorg Chem.* 1975; 14: 2521-2526.
23. Billington DC, Helps IM, Pauson PL, Thomson W, Willison D. The effect of ultrasound and of phosphine and phosphine-oxides on the Khand reaction. *J Organomet Chem.* 1988; 354: 233-242.
24. Park HJ, Lee BY, Kang YK, Chung YK. Stereoselective Pauson-Khand reactions via the chiral $[(alkyne)Co_2(CO)_5\{P(OMe)_3\}]$. *Organometallics.* 1995; 14: 3104-3107.
25. Farrar DH, Lough AJ, Poe AJ, Stromnova TA. Bis[tricarbonyl(triisopropyl phosphite)cobalt](Co-Co) Dichloromethane Solvate. *Acta Crystallogr.* 1995; C51: 2008-2010.
26. Duffy NW, McAdam CJ, Robinson BH, Simpson J. Preparation and redox properties of phosphite derivatives of $R_2C_2Co_2(CO)_{6-n}[P(OMe)_3]_n$ ($R=CF_3, MeO_2C$). *J Organomet Chem.* 1998; 565: 19-28.
27. John McAdam C, Brunton JJ, Robinson BH. Ferrocenylethynyl naphthalenes and acenaphthylenes; communication between ferrocenyl and cluster redox centres. *J Chem Soc Dalton Trans.* 1999; 2487-2496.
28. Haumann M, Meijboom R, Moss JR, Roodt A. Synthesis, crystal structure and hydroformylation activity of triphenylphosphite modified cobalt catalysts. *Dalton Trans.* 2004; 1679 - 1686.
29. Meijboom R, Haumann M, Roodt A, Damoense L. Synthesis, spectroscopy, and hydroformylation activity of sterically demanding, phosphite-modified cobalt catalysts. *Helv Chim Acta.* 2005; 88: 676-693.
30. Knorr M, Jourdain I, Villafane F, Strohmman C. Reactivity of silyl-substituted heterobimetallic iron-platinum hydride complexes towards unsaturated molecules: Part II. Insertion of trifluoropropyne and hexafluorobutyne into the platinum-hydride bond. *J Organomet Chem.* 2005; 690: 1456-1466.
31. Clément S, Guyard L, Knorr M, Dilsky S, Strohmman C, Arroyo M. Ethynyl[2.2]paracyclophanes and 4-isocyano[2.2]paracyclophane as ligands in organometallic chemistry. *J Organomet Chem.* 2007; 692: 839-850.
32. Clément S, Guyard L, Khatyr A, Knorr M, Rousselin Y, Kubicki MM et al. Synthesis, crystallographic and electrochemical study of ethynyl[2.2]paracyclophane-derived cobalt metallatetrahedranes. *J Organomet Chem.* 2012; 699: 56-66.
33. Jourdain I, Knorr M, Strohmman C, Unkelbach C, Rojo S, Gómez-Iglesias P et al. Reactivity of Silyl-Substituted Iron-Platinum hydride complexes toward unsaturated molecules: 4. Insertion of fluorinated aromatic alkynes into the Platinum-Hydride bond. Synthesis and reactivity of heterobimetallic dimetallacylopentenone, dimetallacyclobutene, μ -vinylidene, and μ_2 - σ -alkenyl complexes. *Organometallics.* 2013; 32: 5343-5359.
34. Brieger L, Jourdain I, Knorr M, Strohmman C. Crystal structure of dicarbonyl[μ_2 -methylenebis(diphenylphosphane)- $\kappa^2P:P'$][μ_2 -2-(2,4,5-trimethylphenyl)-3-oxoprop-1-ene-1,3-diy] (triphenylphosphane- κP) ironplatinum (Fe-Pt)-dichloromethane-toluene (1/1/2), $[(OC)_2Fe(\mu-dppm)(\mu-C(=O)C(2,4,5-C_6H_2Me_3)=CH)Pt(PPh_3)]$. *Acta Cryst.* 2019; E75: 1902-1906.

35. Mohamed AS, Jourdain I, Knorr M, Boullanger S, Brieger L, Strohmam C. Heterodinuclear Diphosphane-Bridged Iron-Platinum diyne complexes as metalloligands for the assembly of polymetallic systems (Fe, Pt, Co). *J Clust Sci.* 2019; 30: 1211–1225.
36. Mohamed AS, Jourdain I, Knorr M, Brieger L, Strohmam C. Crystal structure of $\{\mu_2\text{-}1,2\text{-bis}[(4\text{-methylphenylsulfanyl})\text{-}3\text{-oxoprop-}1\text{-ene-}1,3\text{-diyl-}1:2\kappa^2\text{C}3:\text{C}1]\text{dicarbonyl-}1\kappa^2\text{C-}[m_2\text{-methylenebis(diphenylphosphane)-}1:2\kappa^2\text{P:P}'](\text{triphenylphosphane-}2\kappa\text{P})\text{ironplatinum(Fe-Pt),}[(\text{OC})_2\text{Fe}(\mu\text{-dppm})\{\mu\text{-C(=O)C(4-MeC}_6\text{H}_4\text{SCH}_2\text{)=CCH}_2\text{SC}_6\text{H}_4\text{Me-}4\}\text{Pt(PPh}_3\text{)}]\}$. *Acta Cryst.* 2020; E76: 1087-1091.
37. Dolomanov OV, Bourhis LJ, Gildea RJ, Howard JA, Puschmann H. OLEX2: A complete structure solution, refinement and analysis program. *J Appl Cryst.* 2009; 42: 339-341.
38. Sheldrick GM. SHELXT – Integrated space-group and crystal-structure determination. *Acta Cryst.* 2015; A71: 3-8.
39. Sheldrick GM. Crystal structure refinement with SHELXL. *Acta Cryst.* 2015; C71: 3-8.
40. Sumner GG, Klug HP, Alexander LE. The crystal structure of dicobalt octacarbonyl. *Acta Cryst.* 1964; 17: 732-742.
41. Leung PC, Coppens P. Experimental charge density study of dicobalt octacarbonyl and comparison with theory. *Acta Cryst.* 1983; B39: 535-542.
42. Castro J, Moyano A, Pericàs MA, Riera A, Maestro MA, Mahía J. Tris(pyrrolyl)phosphine-substituted Acetylene–Dicobaltcarbonyl complexes: Syntheses, structural characterization, and reactivity studies. *Organometallics.* 2000; 19: 1704-1712.
43. Castro J, Moyano A, Pericàs MA, Riera A, Alvarez-Larena A, Piniella JF. Acetylene–Dicobaltcarbonyl complexes with chiral phosphinooxazoline ligands: Synthesis, structural characterization, and application to enantioselective intermolecular Pauson–Khand reactions. *J Am Chem Soc.* 2000; 122: 7944-7952.
44. Gimbert Y, Robert F, Durif A, Averbuch MT, Kann N, Greene AE. Synthesis and characterization of new binuclear Co(0) complexes with diphosphinoamine ligands. A potential approach for asymmetric Pauson–Khand reactions. *J Org Chem.* 1999; 64: 3492-3497.
45. Choi N, Conole G, King JD, Mays MJ, McPartlin M, Stone CL. Reactions of diarsines with bi- and tri-metallic carbonyl complexes containing cobalt. *J Chem Soc Dalton.* 2000; 395-405.
46. Garçon M, Cabré A, Verdaguer X, Riera A. Synthesis, coordination study, and catalytic Pauson–Khand Reactions of quinoxP*(CO)₄-μ-alkyne dicobalt complexes. *Organometallics.* 2017; 36: 1056-1065.
47. Bott SG, Yang K, Richmond MG. X-ray diffraction structure of Co₂(CO)₄(μ-PhC≡CH)[(Z)-Ph₂PCH=CHPPh₂]: Proof for diphosphine ligand chelation. *J Chem Crystallogr.* 2000; 30: 627-632.
48. Gregson D, Howard JAK. The X-ray single-crystal and molecular structures of [Co₂(CO)₆C₂R₂] for R = Ph (I), CO₂Me (II) (292 K) and R = tert-Bu (III) (200 K). *Acta Cryst.* 1983; C39: 1024-1027.
49. Bird PH, Fraser AR, Hall DN. Reactions of μ-Diphenylethyne-hexacarbonyldicobalt with Bis(diphenylphosphino)methane and Bis(diphenylarsino)methane. Crystal Structures of (tolan)(dpm)Co₂(CO)₄ and (tolan)(dam)₂Co₂(CO)₂*C₂H₄Cl₂. *Inorg Chem.* 1977; 16: 1923-1931.
50. Yang K, Bott SG, Richmond MG. Reversible Chelate-to-Bridge ligand exchange in Co₂(CO)₄(μ-PhC≡CPh)(bma) and Alkyne-Diphosphine ligand coupling. synthesis, reactivity, and molecular structures of Co₂(CO)₄(μ-PhC≡CPh)(bma), Co₂(CO)₄(μ-PhC≡CPh){(Z)-Ph₂PCH=CHPPh₂}, and

$\text{Co}_2(\text{CO})_4\{\eta^2, \eta^2, \eta^1, \eta^1\text{-}(Z)\text{-Ph}_2\text{PC(Ph)=Ph)CC=C(PPh}_2\text{)C(O)OC(O)}\}$. Organometallics. 1994; 13: 3788-3799.



Enjoy *ACR* by:

1. [Submitting a manuscript](#)
2. [Joining in volunteer reviewer bank](#)
3. [Joining Editorial Board](#)
4. [Guest editing a special issue](#)

For more details, please visit:

<http://www.lidsen.com/journals/acr>